Arthritis & Rheumatology
Vol. 0, No. 0, Month 2019, pp 1–11
DOI 10.1002/art.41078

American College of Rheumatology
Empowering Rheumatology Professionals

Neutrophil Extracellular Traps in Tissue and Periphery in Juvenile Dermatomyositis

Bhargavi Duvvuri,[1] Lauren M. Pachman,[2] Gabrielle Morgan,[2] Amer M. Khojah,[2] Marisa Klein-Gitelman,[3] Megan L. Curran,[4] Stephen Doty,[5] and Christian Lood[1]

Objective. Neutrophils are key immune cells participating in host defense through several mechanisms, including the formation of neutrophil extracellular traps (NETs). This study was undertaken to investigate the role of neutrophils in juvenile dermatomyositis (JDM).

Methods. Electron microscopy was used to identify neutrophils in tissue. NETs were also imaged using fluorescence microscopy and quantified using a myeloperoxidase-DNA enzyme-linked immunosorbent assay (ELISA) in plasma obtained from healthy children (n = 20), disease controls (n = 29), JDM patients (n = 66), and JDM patients with history of calcifications (n = 20). Clinical data included disease activity scores and complement C4 levels. Levels of immune complexes (ICs) and calprotectin were analyzed using ELISA.

Results. Using electron microscopy, neutrophils were found to infiltrate affected muscle tissue, engulfing deposited calcium crystals. Uptake of the crystals led to neutrophil activation ($P < 0.01$) and subsequent phosphatidylinositol 3-kinase– and NADPH oxidase–dependent but peptidylarginine deiminase 4–independent formation of NETs, which contained mitochondrial DNA ($P < 0.05$), as confirmed in vivo ($P < 0.001$) and in vitro ($P < 0.01$). Peripheral NET levels were associated with calcinosis ($P = 0.01$), ICs ($P = 0.008$), and interleukin-8 levels ($P = 0.004$). Children with JDM had impaired NET clearance ($P = 0.01$), associated with autoantibody profiles including melanoma differentiation–associated protein 5 ($P = 0.005$), and depressed complement C4 levels ($r = -0.72$, $P = 0.002$). Furthermore, children with JDM showed evidence of neutrophil activation, with elevated levels of peroxidase activity ($P = 0.02$) and calprotectin ($P < 0.01$), which were associated with disease activity ($P = 0.007$), and dyslipidemia (odds ratio 4.7, $P < 0.05$).

Conclusion. We found novel mechanisms of both calcium crystal–mediated neutrophil activation and cell death in JDM pathophysiology. Targeting this pathway may reduce the frequency and extent of calcinosis, as well as prevent long-term development of comorbidities, including atherosclerosis.

INTRODUCTION

Juvenile dermatomyositis (JDM) is a rare vasculopathic disease with an incidence of 3.2 cases per million children each year in the United States (1). Our lack of knowledge concerning disease pathophysiology is accompanied by adverse outcomes: adults who have had JDM in childhood have evidence of premature cardiovascular damage (2). One debilitating manifestation of chronic JDM is calcinosis, the formation of calcium deposits/crystals in soft tissue, which occurs in ~30% of children with JDM (3). Of note, calcifications are most likely to be present in children who experienced a delay in the initiation of therapy and/or cutaneous inflammation, which suggests a critical association between chronic inflammation and calcifications (4).

Neutrophils are key immune cells participating in host defense through several mechanisms, including the formation of neutrophil extracellular traps (NETs), a cell death process in which DNA is extruded together with cytoplasmic and granular content to trap and eliminate extracellular pathogens.

Dr. Pachman's work was supported by the Cure JM Foundation and the Greater Chicago Chapter of the Arthritis Foundation. Dr. Lood's work was supported by the Lupus Research Alliance (grant 519414) and the Cure JM Foundation.

[1]Bhargavi Duvvuri, PhD, Christian Lood, PhD: University of Washington, Seattle; [2]Lauren M. Pachman, MD, Gabrielle Morgan, MA, CCRP, Amer M. Khojah, MD: Cure JM Center of Excellence, Ann & Robert H. Lurie Children's Hospital of Chicago, and Northwestern University Feinberg School of Medicine, Chicago, Illinois; [3]Marisa Klein-Gitelman, MD, MPH: Ann & Robert H. Lurie Children's Hospital of Chicago and Northwestern University Feinberg School of Medicine, Chicago, Illinois; [4]Megan L. Curran, MD, MS: University of Colorado School of Medicine, Aurora; [5]Stephen Doty, PhD: Hospital for Special Surgery, New York, New York.

No potential conflicts of interest relevant to this article were reported.

Address correspondence to Christian Lood, PhD, University of Washington, Department of Medicine, Division of Rheumatology, 750 Republican Street, Seattle, WA, 98109. E-mail: Loodc@uw.edu.

Submitted for publication June 7, 2019; accepted in revised form August 8, 2019.

Although beneficial from the perspective of host–pathogen interaction, exaggerated neutrophil activation and NET formation have been linked to inflammation, cardiovascular disease, and autoimmunity, including rheumatic diseases (5–9). It was recently found that immune complexes (ICs), commonly found in autoimmune conditions, induce NET formation (5). NETs are inflammatory, and they induce interferon (IFN) production through the cyclic GMP-AMP synthase/stimulator of IFN genes (cGAS/STING) pathway and propagate disease in lupus-prone mice (5,10). IFNs are clearly involved in JDM (11), but the potential role of NETs has yet to be determined.

Neutrophils have received very little attention in JDM pathogenesis, likely due to the lack of their identification in JDM muscle biopsies, despite careful scrutiny (12). However, a recent proteomics study showed a "tumor necrosis factor hub" present in JDM neutrophils as compared to those in healthy children, suggesting that neutrophils are affected by the inflammatory environment (13). Further, elevated levels of the neutrophil-derived alarmin calprotectin have been reported in JDM (14). Cell-free DNA has been seen in adult DM in association with interstitial lung disease, though it is not known whether this corresponds to NETs (15,16). Furthermore, whether children with JDM have elevated levels of NETs has not been investigated.

Inasmuch as calcinosis (e.g., calcium crystals) are involved in the pathophysiology of JDM, it is noteworthy to recognize that other crystals, including cholesterol and monosodium urate monohydrate (MSU) crystals, have the capacity to induce NETosis (17,18), and foster the development of atherosclerosis and gout, respectively. Whether calcium crystals could activate neutrophils to undergo NETosis is not known.

In this report, we describe the presence of calcium crystal–mediated NETosis in children with JDM. Briefly, tissue-infiltrating neutrophils engulfed deposited crystals, triggering a phosphatidylinositol 3-kinase (PI3K)– and reactive oxygen species (ROS)–dependent but peptidylarginine deiminase 4 (PAD4)–independent cell death process leading to NETosis. Evidence of neutrophil activation and cell death was also present in the circulation, particularly in patients with calcinosis, and they were associated with markers of disease activity and dyslipidemia. Our results show several novel mechanisms through which neutrophils may contribute to JDM pathogenesis, suggesting possible new therapeutic targets, as well as biomarkers to monitor and potentially predict the development of severe disease outcomes.

PATIENTS AND METHODS

Patients. Children with JDM (n = 66), healthy children (n = 20), and age-matched disease controls (n = 29) were included in the study after age-appropriate informed consent was obtained (Institutional Review Board #2008-13457 and #2001-11715). For patient characteristics, see Supplementary Tables 1–2, available on the *Arthritis & Rheumatology* web site at http://onlinelibrary.wiley.com/doi/10.1002/art.41078/abstract. Myositis-specific autoantibodies (MSAs) were assessed at the Oklahoma Medical Research Foundation Clinical Immunology Laboratory. Calcifications were confirmed by radiography or computed tomography (19). Calcifications were removed surgically and stored at −80°C after removal of adherent connective tissue. Disease activity scores (DAS) (20) were obtained at the time of the physical examination. Neopterin levels were measured as previously described (21). Fasting lipid levels were measured by an enzymatic method using a Cobas instrument.

Electron microscopy. Tissue samples were preserved in 2% paraformaldehyde and 0.5% glutaraldehyde in 0.05*M* cacodylate buffer (pH 7.4) at 4°C for 4–18 hours. Following fixation, the tissues were treated with reduced osmium tetroxide followed by dehydration in ethyl alcohol. The Spurr's resin (Electron Microscopy Sciences) was prepared and mixed 1:1 with propylene oxide and incubated overnight on a rotator. A change of Spurr's resin:propylene oxide at 3:1 was made, and samples were infiltrated overnight. The final embedding was completed in pure Spurr's resin (hard mixture) for 12–18 hours and polymerized at 60°C. Embedded samples were thin-sectioned (60–80 nm thickness) for electron microscopy using a diamond knife (Diatome) on a Reichert Ultracut E and analyzed using a Philips CM-12 transmission electron microscope at 80 kV accelerating voltage. Mineral crystal size and arrangement were studied by tilting the specimen stage through 0–20 degrees of tilt and/or by darkfield imaging (22). Individual crystals could be measured in the darkfield mode and by using the 002 diffraction line from selected-area diffraction.

Neutrophil biomarker assays. Peroxidase activity was analyzed as previously described (5). Levels of calprotectin (S100A8/A9) were analyzed in plasma using a commercial enzyme-linked immunosorbent assay (ELISA) kit according to the instructions of the manufacturer (R&D Systems).

NET assays. Human neutrophils were isolated from heparinized blood using PolymorphPrep, according to the instructions of the manufacturer (Axis-Shield). Isolated neutrophils (1×10^6 cells/ml) were incubated in poly-L-lysine–coated tissue culture plates with or without the following inhibitors: diphenyleneiodonium (25 μ*M*; Sigma), thenoyltrifluoroacetone (1 μ*M*; Sigma), LY294002 (10 μ*M*; Invitrogen), cytochalasin B (5 μ*M*; Sigma), and Cl-amidine (200 μ*M*; Calbiochem). They were incubated for 1 hour prior to addition of the stimuli, e.g., calcium crystals and phorbol myristate acetate (PMA) (20 nm). After incubation with agonist for 4 hours, NETs were detached with micrococcal nuclease (0.3 units/ml; Fisher Scientific) diluted in nuclease buffer containing 10 m*M* TrisHCl (pH 7.5), 10 m*M* $MgCl_2$, 2 m*M* $CaCl_2$, and 50 m*M* NaCl.

Detached NETs were quantified by Sytox green staining (Life Technologies). In addition, NETs were quantified using a myeloperoxidase (MPO)–DNA ELISA, as described previously (5). For fluorescence microscopy, cells were fixed with 4% paraformaldehyde, permeabilized with saponin (Alfa Aesar), and blocked with 1% bovine serum albumin (BSA) in phosphate buffered saline (PBS), prior to staining with detection antibodies. DNA was detected using Sytox green, whereas neutrophil elastase was detected using a polyclonal rabbit antibody (ab21595; Abcam) followed by a secondary Cy5-conjugated goat anti-rabbit antibody (Jackson ImmunoResearch). The cells were visualized using an EVOS cell imaging system (Life Technologies).

NET degradation. To detect NET degradation (23), PMA-induced NETs were stained with Sytox green and subsequently incubated with serum (10%) in nuclease buffer for 60 minutes at 37°C. Varying concentrations of micrococcal nuclease were used as positive controls. NETs were washed between each step. NET degradation was calculated as the relative loss of NETs (Sytox green signal) in each well, using the standard curve as a reference.

Calcium crystals. Basic calcium phosphate (BCP) crystals were synthesized according to published protocols (24). Briefly, 15 ml 0.2*M* NaH_2PO_4 was mixed with 12.5 ml 0.2*M* $CaCl_2$ for 1 hour to form calcium precipitates. The precipitates were washed in water with low-speed centrifugation, followed by incubation overnight with 0.5*N* HCl at a final pH of 9.0 overnight. The precipitates were washed with water 4 times, followed by 70% ethanol and additional water washes. The crystals were resuspended in water and stored at 4°C until used. The surgically removed calcium crystals were fragmented using a mortar and pestle and then washed in water and ethanol, as described above, prior to use.

ELISAs for interleukin-8 (IL-8) and ICs. A 96-well microtiter plate (Corning Clear Polystyrene flat-bottomed, medium binding) was coated with 100 μl of capture antibody (4 μg/ml anti-human IL-8; BioLegend) diluted in PBS and incubated overnight at 4°C. After blocking (1% BSA in PBS), samples were added and incubated overnight at 4°C. For detection, plates were incubated with biotinylated detection antibody (1 μg/ml in blocking buffer), followed by the addition of horseradish peroxidase–streptavidin (BioLegend) for an additional 2 hours at room temperature. The reaction was visualized by the addition of tetramethylbenzidine. The reaction was stopped by addition of 2*N* sulfuric acid, and absorbance at 450 nm was measured with a plate reader. Wells were washed thoroughly 2 times in PBS–Tween between every step. Levels of ICs were assessed using a MicroVue CIC-C1q ELISA according to the instructions of the manufacturer (Quidel).

Mitochondrial and nuclear DNA analysis. DNA was isolated from cell culture supernatants using a Plasma/Serum Cell-Free Circulating DNA Purification Micro Kit (Thorold). The StepOnePlus Real-Time PCR System was used to perform quantitative polymerase chain reaction (PCR). Primer sequences for nuclear gene targets (ribosomal protein lateral stalk subunit P0 [RPLP0]: forward 5'-GGAATGTGGGCTTTGTGTTC-3', reverse 5'-CCCAATTGTCCCCTTACCTT-3') and mitochondrial gene targets (cytochrome c oxidase subunit 2, cytochrome c oxidase subunit II [COXII]: forward 5'-CCCCACATTAGGCTT AAAAACAGAT-3′, reverse 5′-TATACCCCCGGTCGTGTAGC-3′) were reported previously (25). All components of PCR except for primers were provided in Power SYBR Green PCR Master Mix (ThermoFisher). PCR was set up in a volume of 20 μl that had a 1× final concentration of Power SYBR Green PCR Master Mix, 1 pair of primers directed against nuclear or mitochondrial genes at a final concentration of 100 n*M*, 5 μl of DNA, and 3 μl of PCR-grade water. Each PCR was set up using the following thermoprofile: incubation for 2 minutes at 50°C followed by a first denaturation step of 10 minutes at 95°C, and 40 cycles of 95°C for 15 seconds, 55°C (COXII) or 60°C (RPLP0) for 1 minute, and then 60°C for 1 minute. Absolute quantification of gene targets is derived from standard curves built by serial dilution of synthesized nuclear and mitochondrial genes.

Statistical analysis. The Mann-Whitney U test and Spearman's correlation test were used when applicable. For comparisons of frequencies, a chi-square test was used. *P* values less than 0.05 were considered significant. The Bonferroni-Holm correction for multiple comparisons was applied when required.

RESULTS

Neutrophil infiltration in JDM tissue. We readily observed infiltrating neutrophils in inflamed JDM tissue, in particular adjacent to calcified muscle tissue (Figures 1A and B), which suggests chemotactic recruitment to the site of calcification. The neutrophils contained phagocytosed crystals within intracellular vesicles (Figure 1C), as did other infiltrating phagocytes, including macrophages (Figure 1D). The crystalized minerals were fairly homogeneous, 80–120 nm in size, similar to the bone components described previously (26), although the tissue-deposited crystals also formed larger aggregates of considerable size (Figures 1A and B).

NETosis induction by calcium crystals through a ROS- and PI3K-dependent pathway. Given that neutrophils were seen phagocytosing calcium crystals in vivo (Figures 1C and D), we investigated whether such crystals could activate neutrophils to undergo NETosis. Assessing cell surface levels of CD66b, a known neutrophil activation marker, experiments demonstrated the capacity of BCP crystals to activate

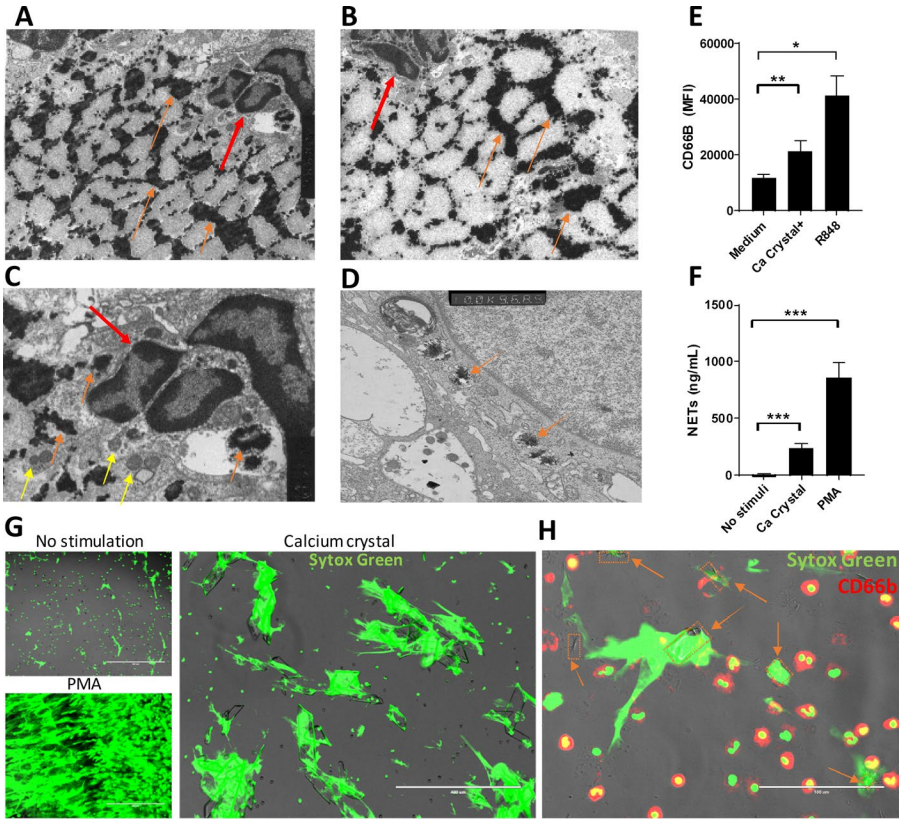

Figure 1. Neutrophil infiltration in the tissue of patients with juvenile dermatomyositis (JDM). **A** and **B**, Muscle tissue (from 2 children with JDM) illustrating calcium deposits (**orange arrows**) and infiltrating neutrophils (**red arrows**). Original magnification × 5,000. **C** and **D**, High-magnification views of a neutrophil engulfing individual and aggregated crystals (magnified view of a portion of **A**) (**C**) and of a macrophage with mineral crystals within vacuoles (**D**). Original magnification × 10,000. **Red arrows** indicate neutrophil lobulated nucleus, **yellow arrows** indicate neutrophil granules, and **orange arrows** indicate calcium crystals. Results are representative of >3 independent experiments. **E** and **F**, Surface expression of CD66b analyzed by flow cytometry (n = 4–6) (**E**) and neutrophil extracellular trap (NET) formation analyzed by fluorimetry (n = 13–15) (**F**). Human primary neutrophils were incubated with synthetic calcium crystals (Ca crystal), Toll-like receptor 7 (TLR-7)/TLR-8 agonist R848, or phorbol myristate acetate (PMA). Bars show the mean ± SEM. **G** and **H**, Fluorescence microscopy staining for DNA using Sytox green (**G**) and CD66b (**H**). Calcium crystals are illustrated with orange boxes and **arrows**. Results are representative of 3 experiments. Bars = 100 μm. * = $P < 0.05$; ** = $P < 0.01$; *** = $P < 0.001$. MFI = mean fluorescence intensity.

neutrophils ($P < 0.01$; Figure 1E). R848, a Toll-like receptor 7 (TLR-7)/TLR-8 agonist, was used as a positive control. To determine whether neutrophil activation proceeded to cell death, we quantified the DNA release using a fluorimetry assay (5,6,10). BCP crystals induced DNA release ($P < 0.001$; Figure 1F), and NETs were apparent when using fluorescence microscopy (Figures 1G and H). Interestingly, only neutrophils in close proximity to the calcium crystals underwent NETosis, whereas neutrophils further away retained a nonactivated phenotype (Figures 1G and H).

NETs can be induced through several distinct signaling pathways, including generation of ROS- and PAD-mediated citrullination of histone H3. PI3K-mediated signaling has previously been shown to be essential in NET formation, acting upstream of NADPH oxidase in generating ROS (10). To investigate the signaling requirements for BCP-mediated NETosis, neutrophils were preincubated with inhibitors blocking pathways known to be involved in NET formation, including PAD2/PAD4, ROS, PI3K signaling, or actin polymerization. Calcium crystal–mediated NETosis was insensitive to PAD inhibition, though PI3K-mediated ROS production was required. This is similar to what has been described for ICs (10), in contrast to neutrophil activation via MSU crystals (found in adult gout patients), which also required PAD activity to induce NET formation (27). Furthermore, neutrophils required actin cytoskeleton activity to undergo calcium crystal–mediated NETosis (Figure 2A). It has recently been shown that NETs contain inflammatory mitochondrial DNA (5,6), which can activate type I IFNs. To determine if calcium crystals induced extrusion of mitochondrial DNA, we analyzed the content of NETs using a quantitative PCR method that assessed levels of nuclear (RPLP0) and mitochondrial (COXII) DNA. Calcium crystals induced the release of both genomic and mitochondrial DNA in a ROS- and PI3K-dependent process ($P < 0.05$; Figures 2B and C). Selective inhibition of mitochondrial ROS reduced mitochondrial DNA release but not that of nuclear DNA (Figures 2B and C). Thus, calcium crystals induced NETosis with

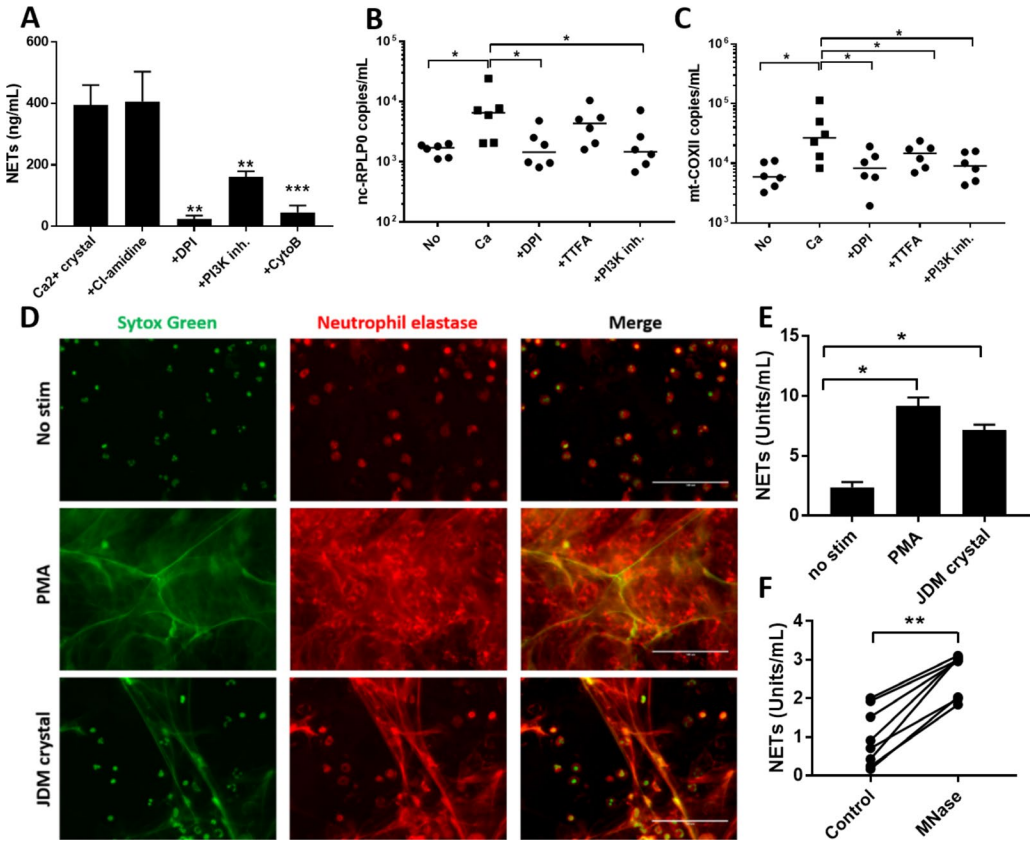

Figure 2. Calcium crystal–mediated NETosis. **A**, Neutrophils were preincubated with inhibitors (inh.) of peptidylarginine deiminase 2 (PAD2)/PAD4 (Cl-amidine; n = 6), reactive oxygen species (ROS) (diphenyleneiodonium [DPI]; n = 8), phosphatidylinositol 3-kinase (PI3K) (n = 8), and cytoskeleton (cytochalasin B [CytoB]; n = 8), prior to addition of calcium crystals and assessment of NETosis by fluorimetry. Bars show the mean ± SEM. ** = $P < 0.01$; *** = $P < 0.001$ versus Ca2+ crystals with no inhibitor added, by Mann-Whitney U test. **B** and **C**, Nuclear ribosomal protein lateral stalk subunit P0 (nc-RPLP0) (**B**) and mitochondrial cytochrome c oxidase subunit II (mt-COXII) (**C**) DNA release, upon calcium crystal–mediated NETosis in the presence of inhibitors targeting ROS (DPI), mitochondrial ROS (thenoyltrifluoroacetone [TTFA]), and the PI3K signaling pathway (n = 6), was assessed by quantitative polymerase chain reaction analysis. Symbols represent individual samples. Bars show the median. **D**, Human primary neutrophils were incubated with crystals that were surgically removed from juvenile dermatomyositis (JDM) patients and analyzed for NETosis by fluorescence microscopy. As a positive control, neutrophils were activated with phorbol myristate acetate (PMA). Results are representative of 3 independent experiments. Bars = 100 μm. **E**, Neutrophils were incubated with crystals that were surgically removed from JDM patients and analyzed for the release of myeloperoxidase (MPO)–DNA (neutrophil extracellular trap [NET]) complexes (n = 6). Bars show the mean ± SEM. **F**, Crystals from JDM patients were either left untreated or treated with micrococcal nuclease (MNase) and analyzed for the release of MPO–DNA complexes by enzyme-linked immunosorbent assay (n = 8). In **B**, **C**, **E**, and **F**, * = $P < 0.05$; ** = $P < 0.01$, by Mann-Whitney U test. No stim = no stimulation.

the release of both mitochondrial and nuclear DNA, in a ROS- and PI3K-dependent but PAD4-independent process.

Crystals isolated from JDM patients are potent NET inducers and contain NET remnants. Given that the BCP crystals could induce NETs in vitro, we next investigated whether tissue-deposited calcium crystals isolated from JDM patients were capable of inducing NETosis. Similar to the BCP crystals, JDM-derived crystals from surgically removed deposits induced NETosis, as was evident by the release of DNA colocalized with neutrophil elastase, as well as MPO–DNA complexes (Figures 2D and E). We then explored whether JDM crystals also induced NETosis in vivo. However, given the difficulty of processing calcified material for immunohistochemistry, we were unable to analyze the crystals by microscopy. Thus, in an attempt to answer this question, purified JDM crystals were treated with micrococcal nuclease to release crystal-bound NETs. As evident in Figure 2F, MPO–DNA complexes were released upon nuclease treatment ($P < 0.01$), which supports the hypothesis that JDM patients developed crystal-bound NETs in vivo.

No evidence of NETosis in the periphery in children with JDM. We examined whether children with JDM showed evidence of NETs in the circulation or in tissues. To investigate this, we analyzed plasma levels of MPO–DNA complexes, a well-established marker of NETosis, in children with JDM and in controls. Though levels of NETs were increased in patients with pediatric systemic lupus erythematosus (SLE) ($P = 0.007$), none

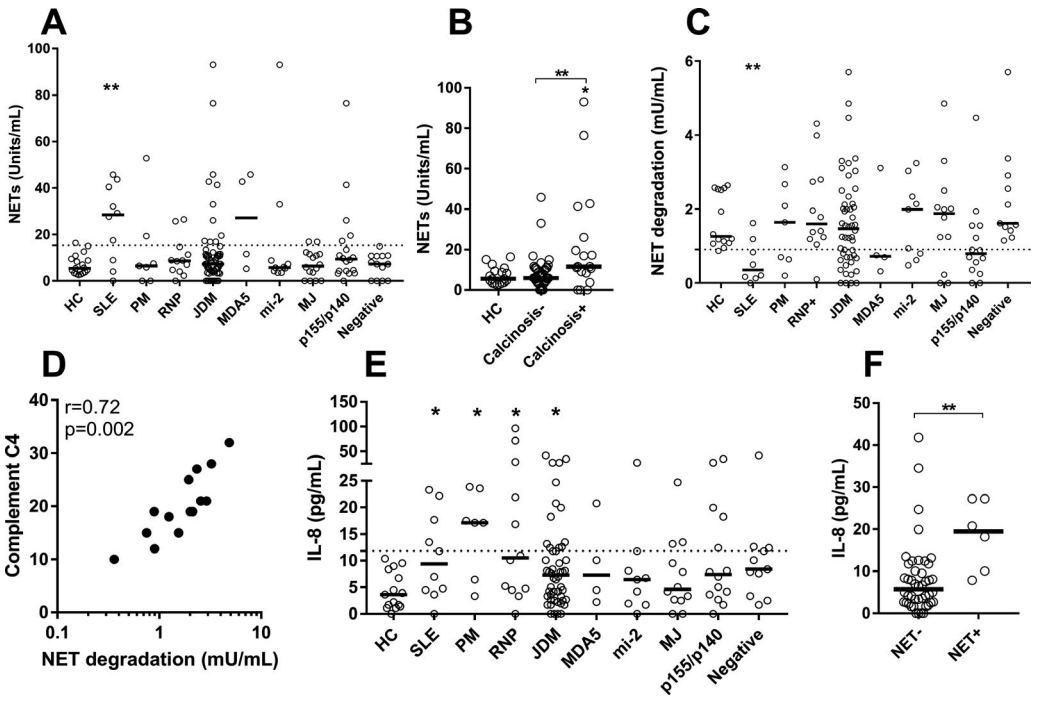

Figure 3. Association of NETosis with calcinosis in JDM. **A**, MPO–DNA complexes (NETs) were measured in different patient groups and compared to the values in healthy children (HC). **B**, NET levels were analyzed in patients without calcinosis (n = 43), patients with calcinosis (n = 18), and healthy children. **C**, NET degradation was assessed in all subjects by in vitro enzymatic assay. **D**, Correlation between levels of complement component C4 and NET degradation (n = 17) was determined using Spearman's correlation test. **E**, Levels of interleukin-8 (IL-8) in all subjects were analyzed by enzyme-linked immunosorbent assay. **F**, IL-8 levels were assessed in patients without circulating NETs (n = 44) and patients with circulating NETs (n = 6). In **A**–**C**, **E**, and **F**, symbols represent individual samples. Bars show the median. The dotted line in **A** represents the 90th percentile of the relevant levels in healthy children, and in **C** and **E**, the dotted lines represent the 10th percentile of these levels. * = $P < 0.05$; ** = $P < 0.01$ versus healthy children or as indicated, by Mann-Whitney U test. SLE = systemic lupus erythematosus; PM = polymyositis; RNP = RNP+ polymyositis; MDA-5 = melanoma differentiation–associated protein 5 (see Figure 2 for other definitions).

of the juvenile myositis groups had elevated levels of NETs (Figure 3A). Given the large variability in NET levels, we investigated whether NETs were associated with certain disease features, including calcinosis. We found that patients with calcinosis had increased levels of NETs compared to JDM patients without calcinosis ($P = 0.009$) and compared to healthy children ($P = 0.02$; Figure 3B).

It was previously shown that SLE patients have reduced degradation of NETs due to low DNase I activity (28). In the present study, there was also a marked impairment in degrading NETs in patients with pediatric SLE ($P = 0.003$; Figure 3C). Similarly, using the 10th percentile of NET degradation in healthy controls as a cutoff, we found that nearly one-third of the JDM patients had an impaired capacity to degrade NETs ($P = 0.01$), particularly patients with MDA-5 and p155/140 MSAs ($P = 0.025$ and $P = 0.024$, respectively, by chi-square test). NET-degrading capacity correlated with complement C4 levels (r = 0.72, $P = 0.002$; Figure 3D). Surprisingly, NET degradation did not correlate with levels of NETs ($P = 0.17$). To investigate whether NETs may contribute to inflammation in JDM, we analyzed levels of the neutrophil chemoattractant IL-8. Levels of IL-8 were elevated in all inflammatory conditions, including pediatric SLE ($P = 0.03$), polymyositis ($P = 0.01$), RNP+ myositis ($P = 0.02$), and JDM ($P = 0.03$; Figure 3E). Importantly, patients with JDM who displayed NETosis had even higher levels of IL-8 ($P = 0.004$; Figure 3F). These data provide evidence that a subgroup of patients with severe JDM have impaired degradation of NETs accompanied by increased circulating levels of NETs, in the presence of ongoing inflammation and calcinosis.

Association of circulating NET levels with ICs. Children with JDM had increased levels of ICs compared to healthy individuals ($P = 0.006$; Figure 4A). Given the well-known contribution of ICs to NET formation in adult SLE, we examined whether levels of ICs correlated with NET levels in pediatric lupus. IC levels correlated strongly with NET levels in pediatric SLE (r = 0.80, $P = 0.01$; Figure 4B), suggesting that similar mechanisms may operate in pediatric and adult SLE. IC levels also correlated with NET levels in JDM patients (r = 0.31, $P = 0.02$; Figure 4C), with NET levels particularly elevated in patients with evidence of circulating ICs ($P = 0.008$; Figure 4D). Patients with JDM, similar to those with pediatric SLE, had circulating ICs that appeared to contribute to heightened NET levels, as observed in a subgroup of the JDM patients.

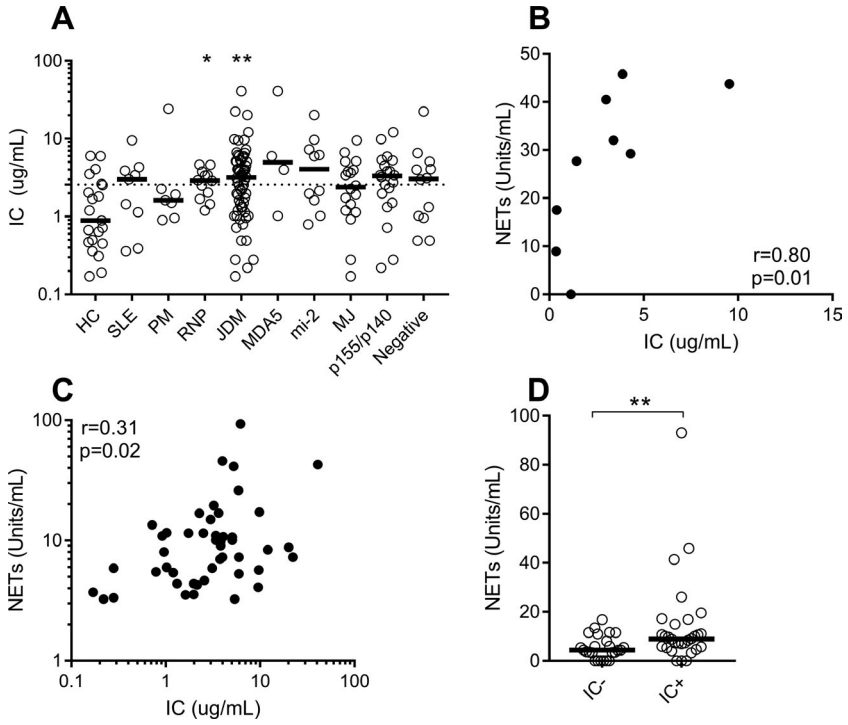

Figure 4. Immune complex (IC) levels in juvenile dermatomyositis (JDM). **A**, IC levels were analyzed by enzyme-linked immunosorbent assay and grouped according to diagnosis and myositis-specific antibodies. The dotted line represents the 75th percentile of the levels in healthy children. * = $P < 0.05$; ** = $P < 0.01$ versus healthy children, by Mann-Whitney U test. **B** and **C**, Correlation between IC levels and neutrophil extracellular trap (NET) levels in pediatric SLE patients (n = 9) (**B**) and JDM patients (n = 55) (**C**) was determined using Spearman's correlation test. **D**, Circulating NET levels were assessed in patients with low levels of ICs (n = 25) and patients with high levels of ICs (n = 30). * = $P < 0.05$; ** = $P < 0.01$, by Mann-Whitney U test. Symbols represent individual samples. Bars show the median. See Figure 3 for other definitions.

Increased neutrophil activation related to disease activity in JDM patients. Given the finding that a subgroup of children with calcinosis demonstrated neutrophil cell death in peripheral blood, we explored whether these children also had evidence of neutrophil activation. To investigate this, we analyzed 2 markers of neutrophil activation in plasma: calprotectin (S100A8/A9) and peroxidase activity. In contrast to previous findings in adult SLE (5), patients with pediatric SLE did not show elevated peroxidase activity (Figure 5A). However, patients with RNP+ myositis and those with JDM showed increased peroxidase activity ($P = 0.01$ and $P = 0.04$, respectively; Figure 5A). Elevated peroxidase activity was observed in patients with high disease activity ($P = 0.02$; Figure 5B) and correlated with markers of inflammation, including the macrophage-derived molecule neopterin (r = 0.45, $P = 0.0007$; Figures 5C and D).

Elevated S100A8/A9 levels in JDM but not in pediatric SLE. It has been reported that serum S100A8/A9 levels are elevated in JDM and associated with disease activity (14). However, S100A8/A9 is released by activated platelets during the clotting process (29,30), which is why serum levels of S100A8/A9 do not reflect physiologic levels of S100A8/A9. In the current study, by using rapidly processed and frozen plasma samples to assess true levels of S100A8/A9 in patient circulation, we found that calprotectin levels were not elevated in patients with pediatric SLE (Figure 5E), even though clearly elevated levels have been demonstrated in adult SLE (31). These data suggest that children may not behave physiologically as young adults and may have a different disease pathophysiology, at least in SLE. In contrast to SLE, pediatric patients with polymyositis, RNP+ myositis, and JDM all showed elevated levels of S100A8/A9 in the circulation ($P < 0.001$, $P = 0.006$, and $P < 0.01$, respectively; Figure 5E). Levels of S100A8/A9 were inversely associated with Childhood Myositis Assessment Scale scores ($P = 0.007$; Figure 5F), suggesting that S100A8/A9 could be a marker of disease activity in JDM. In contrast to neutrophil activation markers, levels of NETs (e.g., neutrophil cell death) were not associated with disease activity in JDM patients (data not shown). Our data demonstrate that JDM patients have ongoing systemic neutrophil activation that is associated with elevated indicators of inflammation and disease activity.

Association of neutrophil activation with dyslipidemia. Neutrophil activation is instrumental in the development of endothelial damage and subsequent atherosclerosis, with elevated levels of S100A8/A9 associated with cardiovascular disease, including in SLE (29,31,32). In the present study,

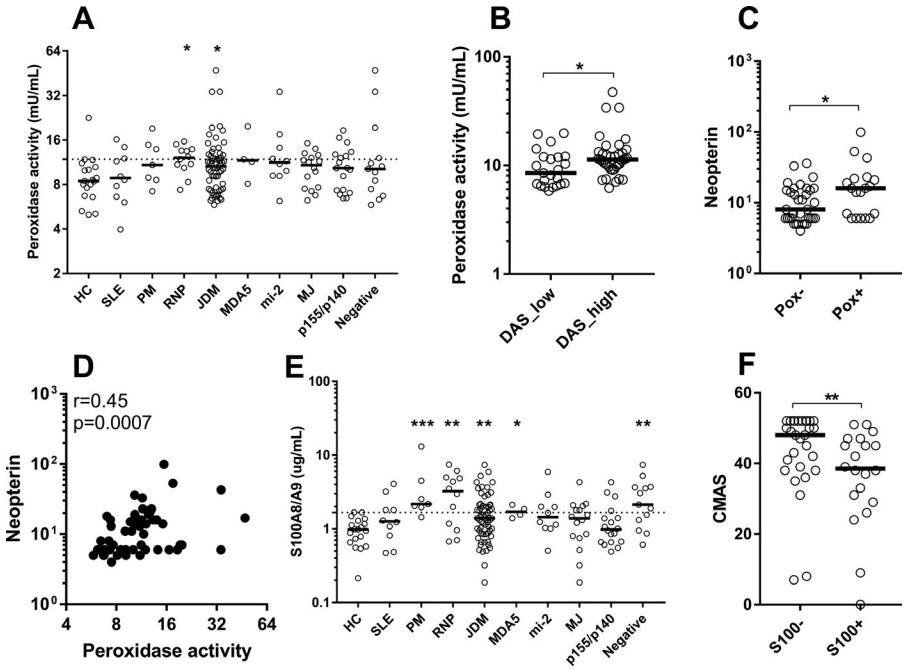

Figure 5. Neutrophil activation markers in juvenile dermatomyositis (JDM). **A**, The neutrophil activation marker peroxidase activity was analyzed in plasma samples from healthy children and from patients with pediatric SLE, PM, RNP, and JDM overall, and JDM subgroups based on myositis-specific antibody positivity. **B**, Peroxidase activity was assessed in plasma samples from JDM patients with low disease activity scores (DAS) (n = 23) and patients with high DAS (n = 38). **C**, Levels of the inflammation marker neopterin were assessed in plasma samples from patients with low peroxidase (Pox) activity and patients with high peroxidase activity. **D**, Correlation between peroxidase activity and neopterin levels in JDM patients (n = 54) was determined using Spearman's correlation test. **E**, The neutrophil activation marker S100A8/A9 was analyzed in plasma samples from all subjects. **F**, The Childhood Myositis Assessment Scale (CMAS) score was determined in JDM patients with low levels of S100A8/A9 (n = 29) and patients with high levels of S100A8/A9 (n = 20). Symbols represent individual samples. Bars show the median. In **A** and **E**, the dotted line represents the 90th percentile of the relevant levels in healthy children. * = $P < 0.05$; ** = $P < 0.01$; *** = $P < 0.001$ versus healthy children or as indicated, by Mann-Whitney U test. See Figure 3 for other definitions.

consistent with prior findings (2,33), JDM patients had low levels of high-density lipoprotein (HDL), with 9 of 23 patients (39%) having dyslipidemia. Furthermore, we observed lipid droplet accumulation in endothelial cells adjacent to muscle fiber, as assessed by electron microscopy. Similar to observations in diabetes mellitus (34), levels of HDL were inversely correlated with calprotectin levels (r = –0.56, $P = 0.01$; Figure 6A) and decreased in children with elevated calprotectin levels ($P = 0.01$; Figure 6B). Finally, elevated levels of calprotectin were associated with dyslipidemia (odds ratio 4.7, $P < 0.05$).

NETs are known to be prothrombotic (35–37), with MPO promoting oxidative modification of HDL and rendering it proatherogenic (38). We found that peroxidase activity, which reflects levels of the main circulating peroxidase, MPO, were inversely correlated with HDL levels (r = –0.44, $P < 0.05$; Figure 6C). Children with high peroxidase activity consistently showed markedly decreased HDL levels ($P = 0.02$; Figure 6D). None of the other markers of disease activity and inflammation (e.g., IC, neopterin, C4, or IL-8 levels) correlated with HDL levels (data not shown), which suggests selectivity in the neutrophil activation markers. Our results indicate that neutrophil activation is associated with a proatherogenic environment in children with JDM.

DISCUSSION

Neutrophils are frontline immune cells that are recruited immediately upon insult through chemotactic signals, which forces them to leave the circulation and migrate into tissue to combat the pathogen. Similar processes occur in sterile inflammation, including rheumatic disease, wherein insults of varying kinds (e.g., IC deposition) result in recruitment of neutrophils into tissue and cause inflammation and organ damage. In this report, we describe the novel finding that neutrophils are present in affected tissue of JDM patients, particularly adjacent to calcified tissue, suggesting that calcinosis-mediated inflammation contributes to chemotactic signaling. Neutrophils and other phagocytes were involved in clearance of the mineral crystals, as demonstrated by endocytosed crystals. The presence of infiltrating neutrophils is novel in JDM; in prior studies, neutrophils were not identified in diagnostic muscle biopsies from children with JDM (12). This discrepancy may

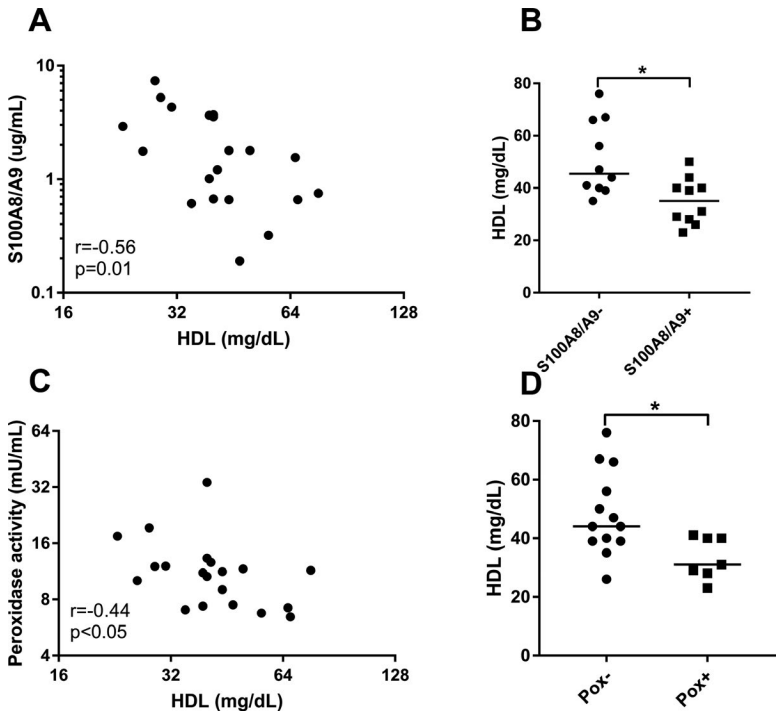

Figure 6. Neutrophil activation markers are associated with dyslipidemia in juvenile dermatomyositis (JDM). **A**, Correlation between levels of calprotectin (S100A8/A9) and fasting levels of high-density lipoprotein (HDL) in JDM patients (n = 20) was determined using Spearman's correlation test. **B**, HDL levels were assessed in patients with high S100A8/A9 levels (n = 10) and patients with low S100A8/A9 levels (n = 10). **C**, Correlation between levels of peroxidase (Pox) activity and fasting levels of HDL in JDM patients (n = 20) was determined using Spearman's correlation test. **D**, HDL levels were assessed in patients with high peroxidase activity (n = 7) and patients with low peroxidase activity (n = 13). In **B** and **D**, bars show the median. * = $P < 0.05$ by Mann-Whitney U test.

be explained by the selection of our patients (e.g., those with calcinosis), but it may also relate to the rapid turnover of neutrophils. Consistent with our findings and similar to what has been observed in SLE and psoriasis (8,39), neutrophils succumb to cell death upon engaging calcium crystal, leaving only remnants of NETs in the tissue.

Interestingly, tissue-infiltrating neutrophils were found to engulf seemingly indigestible crystals in JDM. The interactions of neutrophils with a wide range of crystals, including cocaine crystals, uric acid crystals, mineralo-organic particles, and cholesterol crystals, have been previously described (6,17,18,40). In accordance with findings from prior investigations, we were able to demonstrate that calcium crystals, either BCP or patient-derived crystals, had the capacity to engage neutrophils to induce a process referred to as "frustrated phagocytosis" and subsequent NET formation. Briefly, as elegantly demonstrated by Branzk and colleagues, once the target is beyond the size of being engulfed, the neutrophil will become frustrated and undergo NETosis (41). Similar mechanisms also seem to apply to crystalline size (40). Though most crystals induce NET formation, the underlying signaling requirements are somewhat distinct. Consistent with many previous findings (6,17,18,40), calcium crystals induced NETs in a ROS-dependent process. In contrast, calcium pyrophosphate dehydrate crystals, which are involved in pseudogout, induced NETs in a PI3K-dependent but ROS-independent manner (42). The dependency on PAD-mediated citrullination only applies to MSU and cocaine crystals, whereas cholesterol and calcium crystals induced NETs in a citrullination-independent manner (6,17,18,40).

Further studies are needed to characterize both the common and selective signaling pathways involved in crystal-mediated NET formation. Though neutrophil activation (particularly NETosis) can be targeted pharmaceutically—which has been done successfully in other autoimmune rheumatic diseases such as lupus (5)—understanding mechanisms that act upstream of NETosis (e.g., calcinosis development) would be beneficial in identifying a more attractive drug target that could potentially lead to reduction of general inflammation and not just the neutrophil-dependent component.

Though our experimental data support the hypothesis of calcium crystal–mediated NET formation in the tissue in vivo, low levels of NETs were found in the circulation of JDM patients. These findings indicate that the cell death–inducing component (e.g., calcium crystal) is primarily found in tissue and that NET release is restricted to the site of neutrophil activation. Additionally, calcium crystals may be efficiently neutralized by serum components, reducing their NET-inducing capacity (43). What could then be the source

of peripheral NETs? It has previously been demonstrated that ICs induce NET formation in an Fcγ receptor IIa– and TLR-dependent manner in SLE (5,10). Consistent with those findings, we observed that children with pediatric SLE also had highly elevated levels of NETs, which strongly correlated with IC levels. Notably, elevated levels of ICs were also present in JDM patients and were associated with NET levels. Thus, it is likely that ICs may contribute to activation and death of neutrophils in JDM as well. Though most JDM patients did not have elevated levels of NETs in the periphery, impaired degradation, as described in our study, may still affect the persistence of NETs by promoting inflammation and damaging the vasculature (37,44). In accordance with this hypothesis, NET levels and the capacity to degrade NETs were associated with markers of inflammation, in particular IL-6 levels, in JDM patients. It has previously been demonstrated that NETs (specifically NET-derived mitochondrial DNA) were interferogenic and that they signaled through the DNA-sensing cGAS-STING pathway to induce type I IFNs (5). It is therefore likely that NETs may contribute to the prominent type I IFN signature present in JDM patients (11).

Neutrophil activation, with elevated levels of calprotectin, has been described as occurring in the sera of JDM patients and is associated with disease activity (14). However, given the activation of neutrophils and platelets during the coagulation process that results in the release of calprotectin (29,30), serum levels of calprotectin do not reflect physiologic levels of calprotectin. Our investigation is the first to assess true levels of calprotectin in patient circulation using rapidly processed plasma samples, thereby avoiding the influence of coagulation on immune cell activation. Importantly, we found that calprotectin and peroxidase levels were increased in JDM patients and were associated with markers of disease activity, implicating an important role of neutrophils in JDM pathogenesis and their potential utility as biomarkers to monitor disease progression. Furthermore, neutrophil activation (including NETosis) is detrimental in the development of endothelial damage and subsequent atherosclerosis (35–37), with elevated levels of calprotectin associated with cardiovascular disease (29,31,32), likely through facilitating extravasation and receptor for advanced glycation end products–mediated inflammation (45–47).

JDM patients experience pronounced dyslipidemia early in their disease, as demonstrated in this study, with development of atherosclerosis and increased intima-media thickness occurring during progression into adulthood (2,33). However, the role of neutrophils in the atherosclerotic process of JDM had not previously been addressed. Similar to findings in diabetes mellitus and spondyloarthritis (34,48), we observed that neutrophil activation was associated with dyslipidemia in JDM, which suggests the potential involvement of neutrophils in lipid modulation in JDM. Consistent with this interpretation is the notion that neutrophil-derived MPO promotes oxidative modification of HDL, rendering it proatherogenic (38). Further research, including longitudinal studies, is warranted in order to determine the potential contribution and prognostic value of neutrophil activation and NET formation in dyslipidemia and endothelial dysfunction in JDM.

In conclusion, we have reported on novel mechanisms of calcium crystal–mediated neutrophil activation and cell death in JDM pathogenesis. Targeting this pathway may reduce the disabling consequences of calcinosis and prevent long-term development of comorbidities, including atherosclerosis.

AUTHOR CONTRIBUTIONS

All authors were involved in drafting the article or revising it critically for important intellectual content, and all authors approved the final version to be published. Dr. Lood had full access to all of the data in the study and takes responsibility for the integrity of the data and the accuracy of the data analysis.

Study conception and design. Pachman, Lood.

Acquisition of data. Duvvuri, Morgan, Khojah, Klein-Gitelman, Curran, Doty, Lood.

Analysis and interpretation of data. Duvvuri, Pachman, Lood.

REFERENCES

1. Mendez EP, Lipton R, Ramsey-Goldman R, Roettcher P, Bowyer S, Dyer A, et al, for the NIAMS Juvenile DM Registry Physician Referral Group. US incidence of juvenile dermatomyositis, 1995–1998: results from the National Institute of Arthritis and Musculoskeletal and Skin Diseases Registry. Arthritis Rheum 2003;49:300–5.
2. Eimer MJ, Brickman WJ, Seshadri R, Ramsey-Goldman R, McPherson DD, Smulevitz B, et al. Clinical status and cardiovascular risk profile of adults with a history of juvenile dermatomyositis. J Pediatr 2011;159:795–801.
3. Rider LG, Nistala K. The juvenile idiopathic inflammatory myopathies: pathogenesis, clinical and autoantibody phenotypes, and outcomes. J Intern Med 2016;280:24–38.
4. Pachman LM, Abbott K, Sinacore JM, Amoruso L, Dyer A, Lipton R, et al. Duration of illness is an important variable for untreated children with juvenile dermatomyositis. J Pediatr 2006;148:247–53.
5. Lood C, Blanco LP, Purmalek MM, Carmona-Rivera C, De Ravin SS, Smith CK, et al. Neutrophil extracellular traps enriched in oxidized mitochondrial DNA are interferogenic and contribute to lupus-like disease. Nat Med 2016;22:146–53.
6. Lood C, Hughes GC. Neutrophil extracellular traps as a potential source of autoantigen in cocaine-associated autoimmunity. Rheumatology (Oxford) 2017;56:638–43.
7. Garcia-Romo GS, Caielli S, Vega B, Connolly J, Allantaz F, Xu Z, et al. Netting neutrophils are major inducers of type I IFN production in pediatric systemic lupus erythematosus. Sci Transl Med 2011;3:73ra20.
8. Villanueva E, Yalavarthi S, Berthier CC, Hodgin JB, Khandpur R, Lin AM, et al. Netting neutrophils induce endothelial damage, infiltrate tissues, and expose immunostimulatory molecules in systemic lupus erythematosus. J Immunol 2011;187:538–52.
9. Khandpur R, Carmona-Rivera C, Vivekanandan-Giri A, Gizinski A, Yalavarthi S, Knight JS, et al. NETs are a source of citrullinated autoantigens and stimulate inflammatory responses in rheumatoid arthritis. Sci Transl Med 2013;5:178ra140.
10. Lood C, Arve S, Ledbetter J, Elkon KB. TLR7/8 activation in neutrophils impairs immune complex phagocytosis through shedding of FcgRIIA. J Exp Med 2017;214:2103–19.
11. Baechler EC, Bilgic H, Reed AM. Type I interferon pathway in adult and juvenile dermatomyositis [review]. Arthritis Res Ther 2011;13:249.
12. Wu Q, Wedderburn LR, McCann LJ. Juvenile dermatomyositis: latest advances. Best Pract Res Clin Rheumatol 2017;31:535–57.

13. Frank MB, Wang S, Aggarwal A, Knowlton N, Jiang K, Chen Y, et al. Disease-associated pathophysiologic structures in pediatric rheumatic diseases show characteristics of scale-free networks seen in physiologic systems: implications for pathogenesis and treatment. BMC Med Genomics 2009;2:9.
14. Nistala K, Varsani H, Wittkowski H, Vogl T, Krol P, Shah V, et al. Myeloid related protein induces muscle derived inflammatory mediators in juvenile dermatomyositis. Arthritis Res Ther 2013;15:R131.
15. Peng Y, Zhang S, Zhao Y, Liu Y, Yan B. Neutrophil extracellular traps may contribute to interstitial lung disease associated with anti-MDA5 autoantibody positive dermatomyositis. Clin Rheumatol 2018;37:107–15.
16. Zhang S, Shu X, Tian X, Chen F, Lu X, Wang G. Enhanced formation and impaired degradation of neutrophil extracellular traps in dermatomyositis and polymyositis: a potential contributor to interstitial lung disease complications. Clin Exp Immunol 2014;177:134–41.
17. Warnatsch A, Ioannou M, Wang Q, Papayannopoulos V. Inflammation: neutrophil extracellular traps license macrophages for cytokine production in atherosclerosis. Science 2015;349:316–20.
18. Schauer C, Janko C, Munoz LE, Zhao Y, Kienhöfer D, Frey B, et al. Aggregated neutrophil extracellular traps limit inflammation by degrading cytokines and chemokines. Nat Med 2014;20:511–7.
19. Ibarra M, Rigsby C, Morgan GA, Sammet CL, Huang CC, Xu D, et al. Monitoring change in volume of calcifications in juvenile idiopathic inflammatory myopathy: a pilot study using low dose computed tomography. Pediatr Rheumatol Online J 2016;14:64.
20. Bode RK, Klein-Gitelman MS, Miller ML, Lechman TS, Pachman LM. Disease activity score for children with juvenile dermatomyositis: reliability and validity evidence. Arthritis Rheum 2003;49:7–15.
21. Ibarra MF, Klein-Gitelman M, Morgan E, Proytcheva M, Sullivan C, Morgan G, et al. Serum neopterin levels as a diagnostic marker of hemophagocytic lymphohistiocytosis syndrome. Clin Vaccine Immunol 2011;18:609–14.
22. Bocciarelli DS. Morphology of crystallites in bone. Calcif Tissue Res 1970;5:261–9.
23. Leffler J, Gullstrand B, Jönsen A, Nilsson JÅ, Martin M, Blom AM, et al. Degradation of neutrophil extracellular traps co-varies with disease activity in patients with systemic lupus erythematosus. Arthritis Res Ther 2013;15:R84.
24. McCarthy GM, Cheung HS, Abel SM, Ryan LM. Basic calcium phosphate crystal-induced collagenase production: role of intracellular crystal dissolution. Osteoarthritis Cartilage 1998;6:205–13.
25. Davis MA, Fairgrieve MR, Den Hartigh A, Yakovenko O, Duvvuri B, Lood C, et al. Calpain drives pyroptotic vimentin cleavage, intermediate filament loss, and cell rupture that mediates immunostimulation. Proc Natl Acad Sci U S A 2019;116:5061–70.
26. Eppell SJ, Tong W, Katz JL, Kuhn L, Glimcher MJ. Shape and size of isolated bone mineralites measured using atomic force microscopy. J Orthop Res 2001;19:1027–34.
27. Sabbione F, Keitelman IA, Iula L, Ferrero M, Giordano MN, Baldi P, et al. Neutrophil extracellular traps stimulate proinflammatory responses in human airway epithelial cells. J Innate Immun 2017;9:387–402.
28. Leffler J, Martin M, Gullstrand B, Tydén H, Lood C, Truedsson L, et al. Neutrophil extracellular traps that are not degraded in systemic lupus erythematosus activate complement exacerbating the disease. J Immunol 2012;188:3522–31.
29. Lood C, Tydén H, Gullstrand B, Jönsen A, Källberg E, Mörgelin M, et al. Platelet-derived S100A8/A9 and cardiovascular disease in systemic lupus erythematosus. Arthritis Rheumatol 2016;68:1970–80.
30. Wang Y, Fang C, Gao H, Bilodeau ML, Zhang Z, Croce K, et al. Platelet-derived S100 family member myeloid-related protein-14 regulates thrombosis. J Clin Invest 2014;124:2160–71.
31. Tydén H, Lood C, Gullstrand B, Jönsen A, Nived O, Sturfelt G, et al. Increased serum levels of S100A8/A9 and S100A12 are associated with cardiovascular disease in patients with inactive systemic lupus erythematosus. Rheumatology (Oxford) 2013;52:2048–55.
32. Katashima T, Naruko T, Terasaki F, Fujita M, Otsuka K, Murakami S, et al. Enhanced expression of the S100A8/A9 complex in acute myocardial infarction patients. Circ J 2010;74:741–8.
33. Kozu KT, Silva CA, Bonfá E, Sallum AM, Pereira RM, Viana VS, et al. Dyslipidaemia in juvenile dermatomyositis: the role of disease activity. Clin Exp Rheumatol 2013;31:638–44.
34. Pedersen L, Nybo M, Poulsen MK, Henriksen JE, Dahl J, Rasmussen LM. Plasma calprotectin and its association with cardiovascular disease manifestations, obesity and the metabolic syndrome in type 2 diabetes mellitus patients. BMC Cardiovasc Disord 2014;14:196.
35. Carlucci PM, Purmalek MM, Dey AK, Temesgen-Oyelakin Y, Sakhardande S, Joshi AA, et al. Neutrophil subsets and their gene signature associate with vascular inflammation and coronary atherosclerosis in lupus. JCI Insight 2018;3:99276.
36. Carmona-Rivera C, Zhao W, Yalavarthi S, Kaplan MJ. Neutrophil extracellular traps induce endothelial dysfunction in systemic lupus erythematosus through the activation of matrix metalloproteinase-2. Ann Rheum Dis 2015;74:1417–24.
37. Knight JS, Luo W, O'Dell AA, Yalavarthi S, Zhao W, Subramanian V, et al. Peptidylarginine deiminase inhibition reduces vascular damage and modulates innate immune responses in murine models of atherosclerosis. Circ Res 2014;114:947–56.
38. Smith CK, Vivekanandan-Giri A, Tang C, Knight JS, Mathew A, Padilla RL, et al. Neutrophil extracellular trap–derived enzymes oxidize high-density lipoprotein: an additional proatherogenic mechanism in systemic lupus erythematosus. Arthritis Rheumatol 2014;66:2532–44.
39. Hu SC, Yu HS, Yen FL, Lin CL, Chen GS, Lan CC. Neutrophil extracellular trap formation is increased in psoriasis and induces human β-defensin-2 production in epidermal keratinocytes. Sci Rep 2016;6:31119.
40. Peng HH, Liu YJ, Ojcius DM, Lee CM, Chen RH, Huang PR, et al. Mineral particles stimulate innate immunity through neutrophil extracellular traps containing HMGB1. Sci Rep 2017;7:16628.
41. Branzk N, Lubojemska A, Hardison SE, Wang Q, Gutierrez MG, Brown GD, et al. Neutrophils sense microbe size and selectively release neutrophil extracellular traps in response to large pathogens. Nat Immunol 2014;15:1017–25.
42. Pang L, Hayes CP, Buac K, Yoo DG, Rada B. Pseudogout-associated inflammatory calcium pyrophosphate dihydrate microcrystals induce formation of neutrophil extracellular traps. J Immunol 2013;190:6488–500.
43. Terkeltaub RA, Santoro DA, Mandel G, Mandel N. Serum and plasma inhibit neutrophil stimulation by hydroxyapatite crystals: evidence that serum α_2-HS glycoprotein is a potent and specific crystal-bound inhibitor. Arthritis Rheum 1988;31:1081–9.
44. Knight JS, Subramanian V, O'Dell AA, Yalavarthi S, Zhao W, Smith CK, et al. Peptidylarginine deiminase inhibition disrupts NET formation and protects against kidney, skin and vascular disease in lupus-prone MRL/lpr mice. Ann Rheum Dis 2015;74:2199–206.
45. Ehlermann P, Eggers K, Bierhaus A, Most P, Weichenhan D, Greten J, et al. Increased proinflammatory endothelial response to S100A8/A9 after preactivation through advanced glycation end products. Cardiovasc Diabetol 2006;5:6.
46. Harja E, Bu DX, Hudson BI, Chang JS, Shen X, Hallam K, et al. Vascular and inflammatory stresses mediate atherosclerosis via RAGE and its ligands in apoE$^{-/-}$ mice. J Clin Invest 2008;118:183–94.
47. Hofmann MA, Drury S, Fu C, Qu W, Taguchi A, Lu Y, et al. RAGE mediates a novel proinflammatory axis: a central cell surface receptor for S100/calgranulin polypeptides. Cell 1999;97:889–901.
48. Genre F, Rueda-Gotor J, Remuzgo-Martínez S, Corrales A, Mijares V, Expósito R, et al. Association of circulating calprotectin with lipid profile in axial spondyloarthritis. Sci Rep 2018;8:13728.